Swansea University
Prifysgol Abertawe

Cronfa - Swansea University Open Access Repository

This is an author produced version of a paper published in :
Organic Electronics

Cronfa URL for this paper:
http://cronfa.swan.ac.uk/Record/cronfa34259

Paper:

McGettrick, J., Speller, E., Li, Z., Tsoi, W., Durrant, J. & Watson, T. (2017). Use of gas cluster ion source depth profiling to study the oxidation of fullerene thin films by XPS. *Organic Electronics*
http://dx.doi.org/10.1016/j.orgel.2017.06.022

This article is brought to you by Swansea University. Any person downloading material is agreeing to abide by the terms of the repository licence. Authors are personally responsible for adhering to publisher restrictions or conditions. When uploading content they are required to comply with their publisher agreement and the SHERPA RoMEO database to judge whether or not it is copyright safe to add this version of the paper to this repository.
http://www.swansea.ac.uk/iss/researchsupport/cronfa-support/

Accepted Manuscript

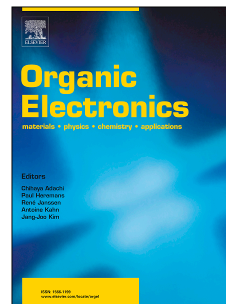

Use of gas cluster ion source depth profiling to study the oxidation of fullerene thin films by XPS

James McGettrick, Emily Speller, Zhe Li, Wing Chung Tsoi, James R. Durrant, Trystan Watson

PII: S1566-1199(17)30279-3

DOI: 10.1016/j.orgel.2017.06.022

Reference: ORGELE 4147

To appear in: *Organic Electronics*

Received Date: 10 February 2017

Revised Date: 7 June 2017

Accepted Date: 11 June 2017

Please cite this article as: J. McGettrick, E. Speller, Z. Li, W.C. Tsoi, J.R. Durrant, T. Watson, Use of gas cluster ion source depth profiling to study the oxidation of fullerene thin films by XPS, *Organic Electronics* (2017), doi: 10.1016/j.orgel.2017.06.022.

This is a PDF file of an unedited manuscript that has been accepted for publication. As a service to our customers we are providing this early version of the manuscript. The manuscript will undergo copyediting, typesetting, and review of the resulting proof before it is published in its final form. Please note that during the production process errors may be discovered which could affect the content, and all legal disclaimers that apply to the journal pertain.

Watson

[1] SPECIFIC, Swansea University, Bay Campus, Swansea. Wales SA1 8EN, UK
*Corresponding Author: Email t.m.watson@swansea.ac.uk, Tel: +44(0) 1792 295509

[2] Centre for Plastic Electronics, Department of Chemistry, Imperial College London, London SW7 2AZ, UK

Abstract

The analysis of organic materials such as phenyl-C61-butyric acid methyl ester ($PC_{61}BM$) by depth profiling is typically fraught with difficulty due to the fragile nature of the sample. In this work we utilise a gas cluster ion source for the controlled depth profiling of organic materials that would historically have been too fragile to analyse and obtain quantitative compositional data through the whole thickness of the film. In particular we examine the oxygen diffusion and photo-oxidation kinetics of one of the most commonly used electron acceptor materials for many organic optoelectronic applications, namely $PC_{61}BM$, in both neat films and in blends with polystyrene. Exposure to AM1.5G light and air under ambient conditions, results in a higher level of surface oxidation of blended $PC_{61}BM$:polystyrene than is observed for either pure control film. Gas cluster ion source depth profiling further confirms that this oxidation is strongest at the extreme surface, but that over time elevated oxygen levels associated with oxidised organic species are observed to penetrate through the whole blended film. The results presented herein provide further insights on the environmental stability of fullerene based organic optoelectronic devices.

Graphical Abstract

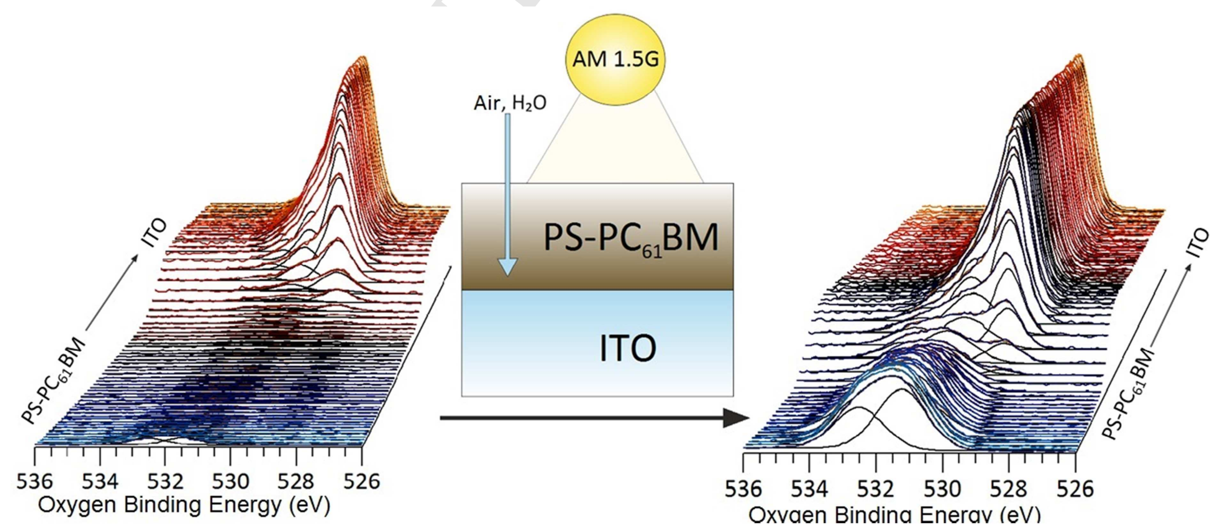

Keywords

OPV, PCBM, Degradation, XPS, GCIS

1. Introduction

ACCEPTED MANUSCRIPT

compatibility with upscaling, and the flexibility of the resultant layers. Whilst most widely used in organic photovoltaics (OPV), it is also used as a component layer in perovskite photovoltaics[1], photodetectors[2] and transistors[3]. Whilst large research efforts have been dedicated to improving the efficiency of such optoelectronic devices, there is a growing concern that their practical use may be limited by their environmental stability, which could in turn limit their commercial exploitation[4–6].

A problem in elucidating the degradation mechanisms of $PC_{61}BM$ has been its *relative* stability compared to other materials present in the device. In many cases relatively rapid degradation of other materials limits the device lifetime[7–9]. Due to this clear degradation, less attention has been paid to the influence of the $PC_{61}BM$ itself, which has often been assumed to be stable. However, it has been noted previously that C_{60} molecules themselves are unstable to oxidation under illumination[10–12].

The structure of $PC_{61}BM$ films becomes extremely complex when the fullerene is blended with a second organic polymer material to form the bulk heterojunction structure typically used in OPV materials[13]. Now multiple phases are present at the surface: fullerene, polymer and fullerene/polymer interfaces or blends, and hence even subtle changes in manufacturing can have profound influence on lifetime[14,15]. Further, even for pure OPV material films, degradation has been noted to vary based on density and as such lifetime is enhanced by ordered crystalline domains[16].

Many studies have previously focussed on bulk techniques for the study of these material systems. In this work we consider a bulk technique to be any that has a penetration depth in the order of >100 nm, i.e. any technique that would be expected to sample the whole ~100 nm thick organic active layer in a single experiment. As such 'bulk' would include all transmission optical techniques such as UV-visible spectroscopy or quantum efficiency measurements. Additionally techniques with penetration depths in the order of micrometres such as Fourier transfer infrared (FT-IR), Raman or energy dispersive X-ray spectroscopy (EDS/EDX) are considered bulk. However, all of these techniques share some extremely advantageous qualities. Firstly, they are experimentally simple, utilising commonly available laboratory equipment and are well understood analytical techniques. Secondly, they often show very strong changes in the device materials, with unambiguous interpretation.

A limitation to these techniques however, is that monitoring the bulk material in such a manner may not accurately reflect the realities of materials where the primary mechanism of device failure is interfacial. For instance, a significant lag in response is expected for the above techniques to monitoring oxidative degradation mechanisms where the oxidation occurs primarily at a surface and gradually penetrates into the bulk. Thus devices might be expected to fail even though no significant changes are observed in the bulk material properties.

Utilising surface techniques such as x-ray photoelectron spectroscopy (XPS), ultraviolet photoelectron spectroscopy (UPS) or surface ion mass spectrometry (SIMS) for the study of organic optoelectronic materials such as $PC_{61}BM$ is expected to offer some benefits in

ACCEPTED MANUSCRIPT

contamination artefacts. Additionally, some effects such as preferential vertical segregation of film components during manufacture might result in this small surface region not accurately representing the bulk material composition.

A classic experiment for XPS or SIMS to negate the influence of surface contaminants or identify variable depth chemistry is to utilise a series of monatomic ion beam etches that strip away the extreme surface of a sample enabling the construction of a depth profile. Such depth profiles have found only limited applicability for OPV materials, however, as depth profiles have historically been prone to an extremely significant problem: some materials, including most organics, are very easily damaged by the incident ion beam used during the etching process. In such cases the incident ions are of sufficient energy to penetrate deep into the material and induce two common experimental artefacts: (a) embedding of incident ions into the material results in a bias to the composition as the incident ions themselves become incorporated into the material of study[25], or (b) the tendency for the studied materials to gradually reduce to a zero oxidation state[26,27]. This second artefact is particularly damaging for the study of OPV materials as organic structures lose oxygen and carbon tends to form graphite-like structures[28]. Even where XPS and SIMS are used to study devices, these artefacts have resulted in complicated experimental design to generate reliable quantitative data[29].

Gas cluster ion sources (GCIS) utilise large clusters of charged ions and are noted in the surface science literature for their relatively mild etching that helps to preserve the materials from experimental artefacts. Typical cluster sizes of ~500 up to several thousand atoms reduce the average kinetic energy of each individual atom in the etching beam from the keV range to the eV range. Molecular dynamics simulations show that craters formed by each individual collision are only a few nm deep with less penetration into the bulk material[30,31].

Although GCIS has been utilised on a wide range of organic systems, the focus has often been on important fundamentals, such as sputter yields [32–34]. However, as the availability of GCIS sources is increasing, more applied studies are possible, such as utilising elemental depth profiles to understand vertical segregation in all-polymer OPV blends[35,36], and these compare well with similar studies using low energy monatomic argon [37]. A particularly strong vein of GCIS-XPS work has been carried out by the Park group who have studied PEDOT:PSS for solar applications including: (1) assessment of the stability of PEDOT:PSS in DSSC electrodes[38]; (2) The energetics of a buried PEDOT:PSS-pentacene interface[39]; (3) A an extension of their work to the energetics PEDOT:PSS-pentacene with an additional $PC_{71}BM$ layer[40]. The above applications share a common requirement for strong structural retention of the residual layers remaining on the substrate during the depth profile and utilise pristine materials.

The study of degradation is potentially even more complex however and has received only limited study in the literature[41]. Prior to degradation materials with high purity are expected to give strong reproducibility and, additionally, the relatively small number of functional groups present initially will minimise peak overlap and broadening in the high resolution XPS spectra. For a highly pure sample of a material such as $PC_{61}BM$, the XPS spectra can be

ACCEPTED MANUSCRIPT

Data analysis is further complicated by the presence of other potentially unstable donors that can degrade alongside the $PC_{61}BM$ material of interest, which generates a need for a stable partner material in order to isolate the role of oxidation of PCBM from other components in the device. Several authors have noted that $PC_{61}BM$ and polystyrene (PS) are readily miscible[42,43] with the addition of PS aiding the formation of stable films, modification of crystal domains[44], simplification of processing[45], or even inclusion in devices to modify morphology[46]. Indeed, additions of PS to $PC_{61}BM$ films are being considered as an advantageous development in their own right for perovskite type solar cells, where the improved quality of the film results in open circuit voltage improvements to the finished device[47]. PS has also long been noted to be stable even under hundreds of hours of accelerated light soaking[48].

In addition to these unknowns, the study of OPV materials during oxidation is traditionally severely hampered during depth profiling with monatomic etching as the oxygen content is impossible to quantify directly due to the large ion beam induced damage to the material being studied.

In this paper we will demonstrate that GCIS-XPS depth profiling can be used to overcome the inherent fragility of materials such as $PC_{61}BM$ as they undergo photo-oxidation in air under 1 sun illumination. We extend the study to a complex blended degrading system of $PC_{61}BM$ with photostable PS, more typical of OPV systems that typically include a polymer/fullerene intermixed phase in addition to the relatively pure fullerene phase. We quantify the introduction of oxygen into the $PC_{61}BM$ film and demonstrate the use of GCIS-XPS analysis to follow the resultant oxidation of the film bulk as a function of time.

ACCEPTED MANUSCRIPT

Inc.). In a typical experiment 24 mg/ml of $PC_{61}BM$ was dissolved in chloroform (Sigma Aldrich). Where PS- $PC_{61}BM$ films are used, 8 mg/ml PS was first dissolved in chlorobenzene (Sigma Aldrich) and $PC_{61}BM$ powder added such that 40% (w/w) $PC_{61}BM$ is present in the final film. The solutions were then coated onto indium tin oxide (ITO) coated glass substrates (KINTEC Company) by spin coating. Typically 35 µl of solution was spun at 800 RPM for 60 s, under 2000 RPM/s acceleration. After the subsequent depth profiling by XPS the film thickness of all samples was confirmed using a Dektak 150 stylus profilometer, which indicated a film thickness of 96 ± 9 nm across the whole population. Photo-aging experiments under the laboratory ambient atmosphere was carried out by placing the samples under a solar simulator of 0.93 Sun AM1.5G (with a KG5 filter) illumination under laboratory ambient conditions (25 ± 3 °C, 37 ± 4 % relative humidity) and exposing samples for the times noted in the text (Figure 1a). The temperature of the films was measured in situ as 34-37 °C using a type K thermocouple, with the relative humidity in the solar simulator measured as 12 ± 1 %. No barrier films were present to protect the organic film. In order to limit external contamination all samples were prepared in a glove box, transferred to a sealed solar simulator and transferred into the XPS with minimal handling and avoiding plastic tools/containers.

XPS measurements were carried out on an Axis Supra instrument (Kratos Analytical, UK) using a monochromated Al K_{α} source with a 15 mA emission current and total power of 225 W, which gives ~ 300 x 700 µm analysis area. The instrument work function is calibrated via Ag, Au & Cu standards. The integral charge neutraliser was used as a default, although samples were mounted with the ITO connected to ground in order to minimise potential charging issues. A sharp main C(1s) peak (FWHM ~0.8-0.9 eV) is typically observed at 284.0 eV for a pristine $PC_{61}BM$. For degrading samples in particular charge correction to this position is sometimes required. In all cases wide scans with a pass energy of 160 eV were recorded, followed by high resolution data with a pass energy of 20 eV, 0.1 eV step size and dwell time of 250 ms.

During depth profile experiments, the base pressure in the instrument is typically ~5 x 10^{-9} Torr, with the pressure in the analysis chamber rising as Ar is introduced into the chamber. In a typical experiment the beam energy and cluster size were set as noted in the text, and set to raster over a 2 x 2 mm area. The Kratos Minibeam 6 Gas Cluster Ion Source is equipped with a Wien filter that prohibits any clusters with mass <50 atoms exiting the gun, and gives a typical Gaussian distribution with FWHM of ~10% of the mass (±25 atoms in this instance). The cluster source is typically optimised for etching with 10 kV Ar^{+}_{500} clusters and gave an ion beam current of 12.7 nA. For the full film depth profiles 2.5 kV Ar^{+}_{500} clusters were used, with a measured ion beam current of 3.6 nA. In order to limit contributions from outside the crater, a 110 µm diameter aperture is used on the detector side of the instrument, and the pass energy increased to 40 eV to compensate for the resultant loss of signal. After a period of etching, typically 30-90 s, high resolution data were recorded and the process repeated (Figure 1b). One sweep is sufficient to collect C(1s) data, and three sweeps for O(1s). Appearance of In(3d) peaks and the emergence of a third low energy O(1s) peak is taken to indicate that the buried ITO has been reached and the experiments are terminated at this point. In order to account for any etch rate variability, the crater depths

ACCEPTED MANUSCRIPT

Quantification was carried out using CasaXPS (version 2.3.17dev6.4k), using Shirley backgrounds. For simplicity the GL(30) lineshape is retained when analysing depth profiles as it better represents the degrading materials that form the bulk of data in this paper. It should be noted however that a lineshape with a higher Lorentzian component, e.g. GL(70) – GL(80) will more adequately models the edge of the pristine $PC_{61}BM$ between ~283-282 eV. We also initially constrained the *relative* positions of peaks in the O(1s) and C(1s) envelopes as observed elsewhere[49], noting that our main C(1s) peak is observed at 284.0 eV and not 285.3 eV. Similarly, the FWHM of the photoelectron peaks, not including the broad high energy π-π* shake up feature, were initially constrained so that all were equal. As materials degrade the various observed peaks become extremely broad due to the multiplicity of chemical environments that develop, and the constraints on the synthetic components have to be relaxed slightly to fit to the experimental data. The C_xH_y peak at 284.8 eV, that represents contributions from the $PC_{61}BM$ side chain and PS polymer chain, requires tight positional and FWHM constraint in all models however to prevent excessive shifting and broadening.

Attenuated total reflection – Fourier transform infrared (ATR-FTIR) spectra were acquired on a FTIR spectrometer (Perkin Elmer Frontier) with a Germanium ATR top plate with crystal diameter 1.3 mm. 1 x 1 cm photo-aged films were removed from the substrate and placed directly onto the ATR crystal for analysis. The spectra were processed from raw data that consisted of 64 scans and 1 cm^{-1} resolution. The spectra were baseline corrected in the Spectrum 10 software. Subsequently, the FTIR absorbance of the ester stretch of the $PC_{61}BM$ side chain at 1737 cm^{-1} was used to normalise the data.

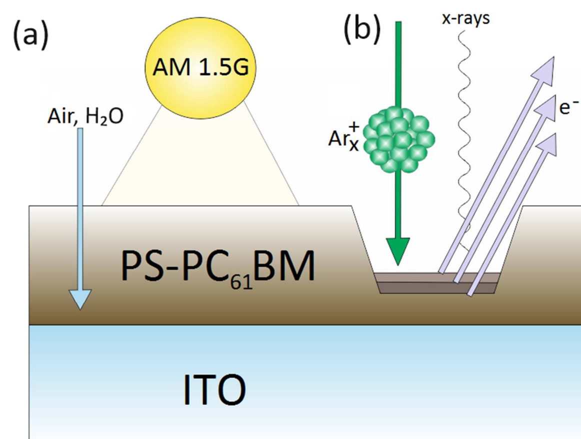

Figure 1. Schematic of a typical experiment (a) $PC_{61}BM$ or PS- $PC_{61}BM$ films are exposed to AM1.5G light under laboratory ambient conditions, which results in degradation (b) Various argon beams are used to etch the substrate, gradually removing top layers to expose underlying materials.

ACCEPTED MANUSCRIPT

the top surfaces of pristine and aged $PC_{61}BM$ are presented in Figure 2. For fresh, as-produced, $PC_{61}BM$ surfaces a sharp main peak centred at 284 eV is observed, along with several smaller peaks (Figure 2a and Table 1). These have previously been observed in synchrotron studies as being from the oxygenated carbon species in the ester group on the $PC_{61}BM$ side-chain, with the broad $\pi \rightarrow \pi^*$ loss peak that is characteristic of sp^2 hybridised systems[49]. A slight excess of O=<u>C</u>-O is noted over the expected 1.4%. This excess is believed to be due partly to contamination (see later Section 3.2) and partly due to the presence of the overlapping loss peak. After photo-aging in air for 1920 min (Figure 2d), the sharp C_{60} peak is still dominant, although broadened peaks attributed to oxidised carbon species in the high energy tail are now more prominent. Unfortunately, it is not possible to differentiate oxidation of the C_{60} cage from oxidation of the side-chain based purely on XPS data. Similar results are obtained for the PS-$PC_{61}BM$ model system initially (Figure 2b), although the influence of aging is more stark as the main 284 eV peak is significantly less dominant, and there is a significant increase in the oxidised carbon species on aging (Figure 2e) compared to $PC_{61}BM$. This is a surprise, as the PS has been selected for its stability under the conditions of study, and control experiments with photo-aged PS films do not result in significant oxidation (Figure 2c, 2f). Thus, whilst the PS-$PC_{61}BM$ system is expected to oxidise *less* than a pure $PC_{61}BM$ film, surface data suggest that it is oxidising more than either component individually.

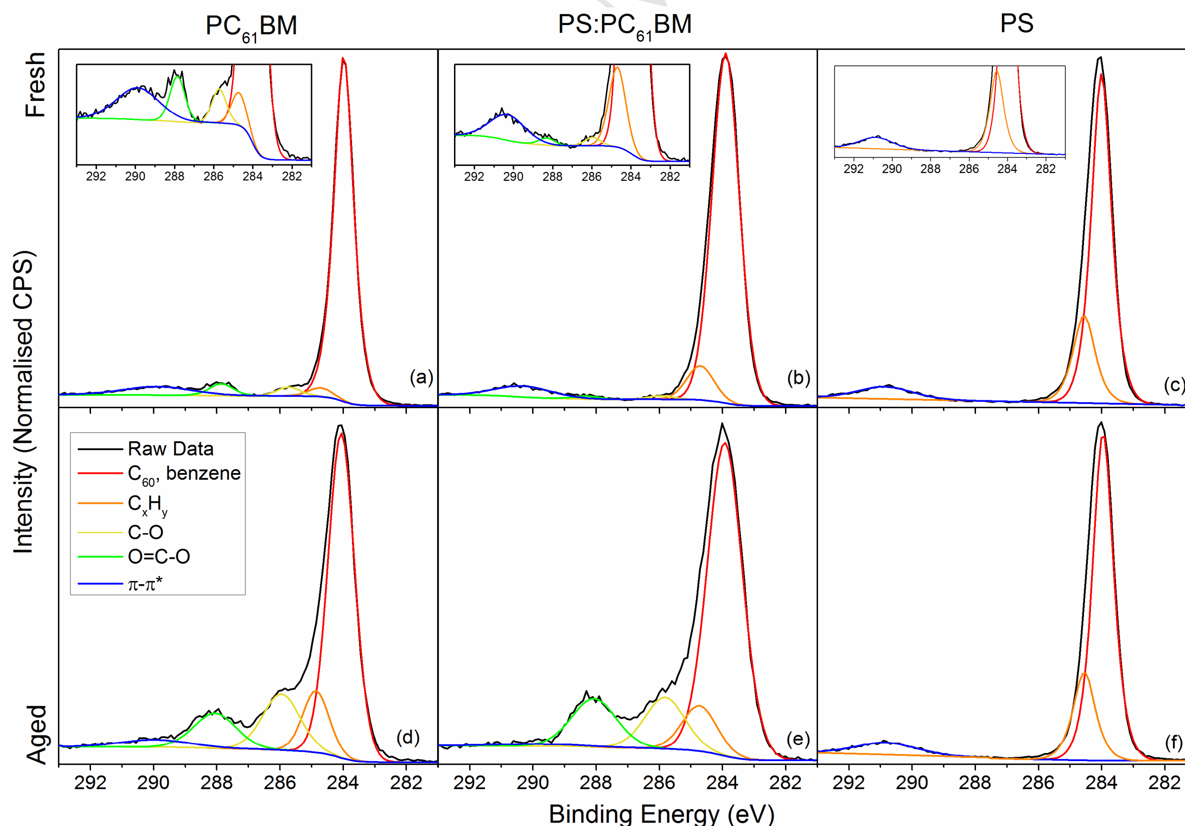

Figure 2. Typical C(1s) envelopes at the surfaces of $PC_{61}BM$ materials. Top row: fresh films of (a) $PC_{61}BM$, (b) PS-$PC_{61}BM$, (c) PS. Second row: films aged for 1920 min light soaking in

			Typical Compositions (Atomic %)				
Element	Position (eV)	Assignment	Predicted $PC_{61}BM$	Fresh $PC_{61}BM$	1920 min Aged $PC_{61}BM$	Fresh PS-$PC_{61}BM$	1920 min Aged PS-$PC_{61}BM$
C(1s)	284.0	C_{60}	89.2	84.0	75.1	82.1	39.0
C(1s)	284.8	C_xH_y	5.4	4.8	6.1	10.2	14.8
C(1s)	286.1	$\underline{C}$-O	1.4	1.6	4.4	1.0	12.4
C(1s)	288.3	O=$\underline{C}$-O	1.4	2.9	4.6	0.4	10.9
C(1s)	289.9	$\pi \rightarrow \pi^*$	-	4.4	5.4	4.9	3.0
O(1s)	529.4	ITO substrate	N/A	not observed	not observed	not observed	not observed
O(1s)	531.1	C-$\underline{O}$-C	1.4	1.1	1.9	0.8	11.4
O(1s)	532.6	C=$\underline{O}$	1.4	1.1	2.4	0.6	8.5

Table 1. Typical C(1s) and O(1s) envelope peak fittings for the surface of $PC_{61}BM$ materials.

No significant shift of the peaks is observed in the O(1s) envelope, which is primarily defined by the two peaks for the ether-like and carbonyl oxygen atoms in the ester group on the $PC_{61}BM$ side chain (Table 1). Although two separate oxygen environments are observed in the O(1s) envelope, it should be noted that only very low levels of oxygen are generally observed for either $PC_{61}BM$ or the PS-$PC_{61}BM$ system before aging. The surface oxidation after photo-aging is particularly pronounced for the PS-$PC_{61}BM$ model system, where the surface oxygen content is 1.4 At% initially and rises to 19.9 At% on aging. A smaller increase in the oxygen content from 2.2 At% to 4.3 At% is observed on aging of $PC_{61}BM$ alone. It should be noted that the combination of increased oxygen signal with the corresponding increase in oxidised species at 286.1 & 288.3 eV in the C(1s) envelope confirms that the organic species are oxidising in both cases, and that the increase in oxygen signal is not due to simple adsorption of oxygen into the organic matrix.

Given the unexpectedly high levels of photo-oxidation in the PS-$PC_{61}BM$ data, the surface was monitored as a function of time (Figure 3). After remaining stable for 120 mins, the surface O(1s) signal is again observed to increase markedly on sample photo-aging, and a low level, noisy N(1s) peak is also noted (Figure 3a & b). Again, the increase in total oxygen is matched by increases in the oxidised carbon components at 286.1 & 288.3 eV in the C(1s) envelope, which confirms oxidation rather than adsorption. The two initial low intensity O(1s) peaks observed in the $PC_{61}BM$ become a single strong broad signal on aging, which suggests multiple similar chemical states may be present for oxygen. Unfortunately, it has been previously calculated that a wide range of O(1s) peak positions are possible depending on the location of the oxidation on the $PC_{61}BM$ molecule[50], with similarly complex results also previously noted for the oxidation of $PC_{71}BM$[17]. This suggests that the simple two peak fitting of the O(1s) envelope used in Table 1 is a significant simplification of the true complex system once oxidation has occurred.

ACCEPTED MANUSCRIPT

$PC_{61}BM$, they note a series of mass fragments with m/z 910 + n*16, where n=1-8, suggesting that up to eight additional oxygen atoms are present on the $PC_{61}BM$ molecule and that the extremely high level of oxygen observed could be consistent with oxidation of the C_{60} cage itself[51]. Unfortunately MALDI requires dissolving the whole film for MS study, so oxidation at the surface vs. the bulk cannot be differentiated. An extensive synthesis by Xiao *et al* also demonstrates that the cage itself possesses a rich potential for functionalisation and eventual opening under mild conditions once initial oxidised species are generated[52]. The current authors suggest that under such conditions severe damage would be expected to the structure of the materials and that the disruption of the C_{60} cage in particular would be expected to have a profound detrimental effect on the molecular orbitals in the molecule and hence on the performance in a full optoelectronic device.

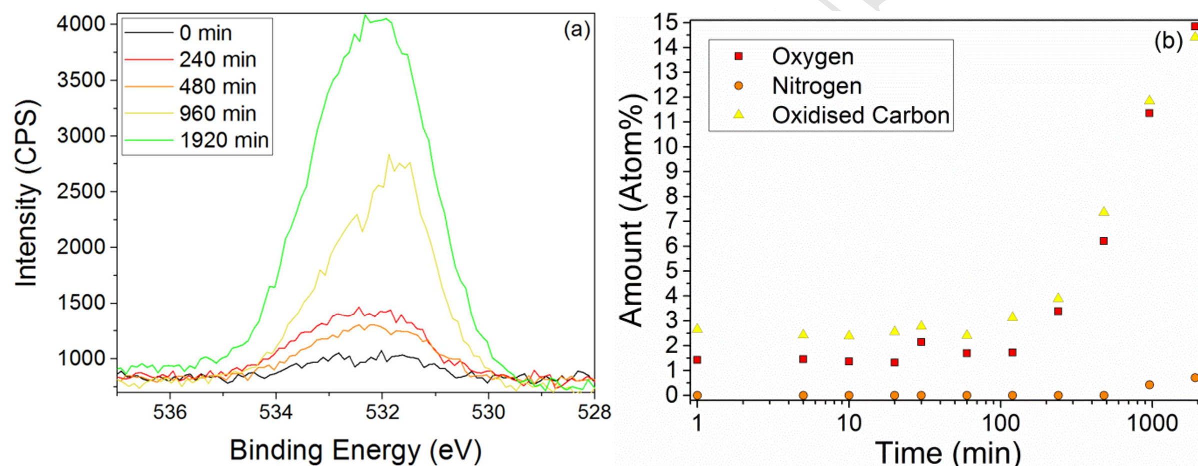

Figure 3. Relationship between the surface oxidation and the duration of light soaking for PS-$PC_{61}BM$. (a) Evolution of the O(1s) envelope and (b) surface elemental concentrations of oxygen, nitrogen and oxidised carbon species.

The PS-$PC_{61}BM$ layers were also examined by FTIR (Figure 4), which confirmed significant changes to the $PC_{61}BM$ molecule. The carbonyl region shows evolution of a shoulder at ~1780 cm^{-1} and a more general broadening of the $PC_{61}BM$ ester carbonyl. Previously a study of $PC_{61}BM$ and C_{60} photodegradation[10] has shown changes in this region are due to the appearance at 1782 cm^{-1} and 1745 cm^{-1} of a broad double degradation peak in addition to the strong initial $PC_{61}BM$ ester peak at 1737 cm^{-1}. Given that the 1782 cm^{-1} peak grows consistently, and given that the appearance of broad hydroxyls in the 3500-3000 cm^{-1} region is only occasional and inconsistent, this is assumed to be a strained ring ketone. Additionally the peaks in this region have been observed to increase in intensity over time for similar systems under photo-aging [18]. The change is pronounced for PS-$PC_{61}BM$, which again suggests significant degradation. Under identical photo-aging conditions, PS shows little surface oxidation and no bulk oxygen content by XPS. It can also be seen in Figure 4 that the sharp peaks associated with the aromatic side chain in the polystyrene[53] at 1601 cm^{-1}, 1584 cm^{-1} and 1542 cm^{-1} are retained, albeit atop an increasingly complex baseline as time progresses.

ACCEPTED MANUSCRIPT

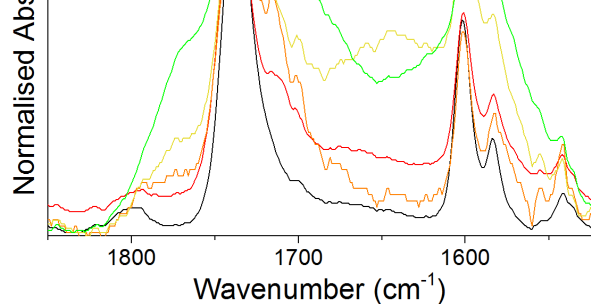

Figure 4. Evolution of carbonyl peaks during photo-aging in air for PS-PC$_{61}$BM films as measured by ATR-FTIR.

3.2 GCIS-XPS Depth Profiling of Organic and Blend Films

The relative similarity of the XPS surface data with the FT-IR bulk data suggests that the oxidation has proceeded considerably. If a diffusion limited hypothesis is correct then it is implied that oxygen diffuses into the bulk of a blended PS-PC$_{61}$BM system relatively quickly. To further examine this, GCIS was used to examine the oxygen penetration into the film bulk by producing a depth profile through the organic layers.

Initially it was necessary to confirm that a PC$_{61}$BM film could be consistently etched without loss of structure. As expected, PC$_{61}$BM etched with a monatomic 5 keV Ar^+ beam does indeed show significant loss of oxygen. Lower energy 0.5 kV Ar^+ etching shows much better structural retentionwith 2.26 % oxygen retained (Table 2 and Figure S1), confirming that low energy monatomic argon etches are effective in reducing, but not completely eliminating, ion beam induced damage in organic systems[37]. This can be contrasted with the gas cluster modes which gradually show a greater structure retention in the C(1s) high energy tail and a sharpening of the main C60/benzene contribution at 284 eV. By contrast there is a clear loss of the C-O, O-C=O and $\pi \rightarrow \pi^*$ contributions at higher acceleration voltages (Figure 5). At the same time, gradually smaller contributions from O(1s) are seen with higher acceleration voltages. The oxygen content of the 2.5 kV Ar^+_{500} etched sample is 2.66 At%, which compares well with the 2.70 At% expected from the PC$_{61}$BM structure, with little chemical reduction of the carbon. Indeed, the 5 kV and 2.5 kV acceleration voltages actually show an increase in the amount of surface oxygen compared to the unetched sample, which is attributed to the removal of adventitious surface carbon contaminants present in the as produced film. Argon inclusion in the etched film is observed for the monoatomic 5 kV Ar^+ beam, and also to a lesser degree with the higher acceleration voltages applied to Ar^+_{500} clusters. The relatively mild etches allowed by gas cluster sources are ideal for organic systems that are often severely damaged by incident Ar^+ beams [28,40,54], although it should be noted that the low energy per Ar atom will also give reduced etch rates compared to higher energy beams. The improved structural retention preserves the subtle quantitative information and allows GCIS argon cluster sources to perform experiments that were previously impossible – one such experiment is following oxidation as it moves through an organic material.

ACCEPTED MANUSCRIPT

ACCEPTED MANUSCRIPT

		Produced	Ar^+	Ar^+					
O	2.70	2.20	0.99	2.26	0.51	0.81	1.71	2.48	2.66
C	97.3	97.8	97.7	97.7	99.5	99.1	98.3	97.5	97.3
Ar	0	N/A	1.30	N/A	0.04	0.06	N/A	N/A	N/A

Table 2. Surface stoichiometry of a fresh $PC_{61}BM$ film after five minutes exposure to typical argon etching beams.

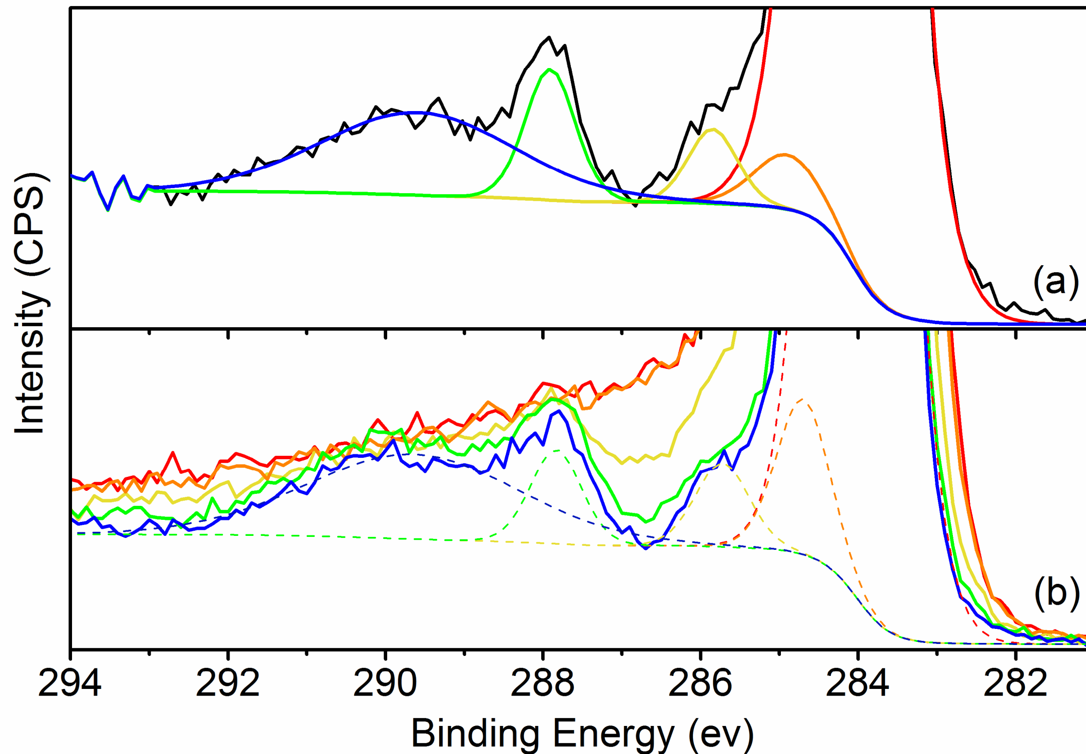

Figure 5. Detail showing evolution of the C(1s) envelope with decreasing acceleration voltage for Ar^+_{500} clusters. (a) A shows a typical $PC_{61}BM$ surface and synthetic components prior to etching (b) The surface after 300 s Ar^+_{500} cluster etching with 20 kV (red), 15 kV (orange), 10 kV (yellow), 5 kV (green) and 2.5 kV (blue). Dashed lines represent the synthetic components after 300 s etching with 2.5 kV clusters – note the reduction of the O-C=O component which indicates its surface excess is in part due contamination.

bulk strongly resemble the PS-$PC_{61}BM$ observed previously (Figure 2b), and little oxygen is observed until the onset of the ITO O(1s) signals from the substrate at a depth of 85 nm (Figure 6b, 7). By contrast much higher oxygen levels are observed in the bulk PS-$PC_{61}BM$ after 1920 min photo-aging in air (Figure 6c,d, 7). The bulk composition of the layer is profoundly altered by considerable oxygen ingress into the material. Initially adventitious surface contamination is removed, resulting in an increase in the observed oxygen signal. After 480 mins exposure to AM1.5G light, there is only a subtle bulk change, but with longer exposure the amount of oxygen in the bulk film increases, particularly close to the top surface of the PS-$PC_{61}BM$. The individual spectra closer to the buried ITO interface tend to be more PS-$PC_{61}BM$-like, suggesting that the degradation is most severe at the top surface and that the limited ingress of oxygen into the bulk prevents more severe damage as depth increases. Additionally, no evidence is noted of degradation of the underlying ITO layer, or of indium migration into the organic film which has been reported as indicating an ITO failure mechanism[55].

Interestingly, for 1920 minute photo-aged PS or $PC_{61}BM$ layers this same scale of oxidation is not observed in the bulk. No O(1s) signal is observed at all for PS below the top surface with only a minor increase in O(1s) signal for $PC_{61}BM$ to 3.9 ± 0.5 At% below the top surface, which suggests that the PS-$PC_{61}BM$ blended film is less stable than either PS or $PC_{61}BM$ individually. Pristine $PC_{61}BM$ films have previously been observed to form aggregated clusters which shrink in size when blended with PS, and also that some $PC_{61}BM$ clusters are entrapped within polystyrene composites[42,46] which would provide additional interfaces that could be attacked. The extremely complex and extended interfaces formed between different domains in the polymer blends typically used in OPV devices offer a ready potential pathway for oxygen (and nitrogen) ingress into blended films that is not available to either pure material. Morphological control of blended materials for OPV is a significant field in its own right, with the morphology of films sensitive to numerous factors such as subtle chemical or physical interactions between the various components and various kinetic or thermodynamic parameters during manufacture[13]. It is also interesting to note that previous work on degradation via GCIS did not observe the same level of oxidation, although this previous study looked at light and oxygen/humidity separately, rather than photo-oxidation in air[41].

$PC_{61}BM$ photo-oxidation in optoelectronic devices, particularly the high oxidation observed in the blended structures representative of OPV devices, has important implications for device stability. Indeed $PC_{61}BM$ remains widely used in OPV, and as a layer in perovskite PV devices due to its simple application via spin coating, low temperature processing, high device efficiency, but all of these positive characteristics are moot for industrial scale up if the material itself is unstable. Even in blend systems where the $PC_{61}BM$ is observed to improve the lifetime, photo-oxidation is still observed and DFT suggests a drop in the LUMO even where the C_{60} cage remains intact[51] and, given demonstrated C_{60} cage opening after heavy oxidation under synthetic chemistry conditions[52], it is plausible that even this assumption underestimates the damage to the molecule. Finally, it should be noted that analysis of films in isolation will not represent the full spectrum of either device protection or

ACCEPTED MANUSCRIPT

whilst the reaction of oxygen *within* a film occurs over minutes[56]. This diffusion limitation is evident both in 1) the observed preferential reaction of the surface and relatively slow penetration into the bulk blended films, and 2) the relatively surface limited oxidation in pure materials.

Ultimately, fine control of manufacturing parameters to limit oxygen ingress and improve the lifetime OPV devices is beyond the scope this paper, but its potential importance is underlined by the observed deep penetration of oxygen into the bulk PS-$PC_{61}BM$ film. GCIS-XPS has a wide potential to be applied to both organic material oxidation and morphology as it eliminates experimental artefacts and allows quantitative studies to be performed. Hence, over several batches of films aged to ~1920 min up to 20 At% oxygen was observed deep into the bulk of PS-$PC_{61}BM$, presumably depending on subtle morphological variability during manufacture. Eliminating such material degradation will be critical for device survival in real world environments, and the subtle control of GCIS methods opens a new viable route to quantification.

ACCEPTED MANUSCRIPT

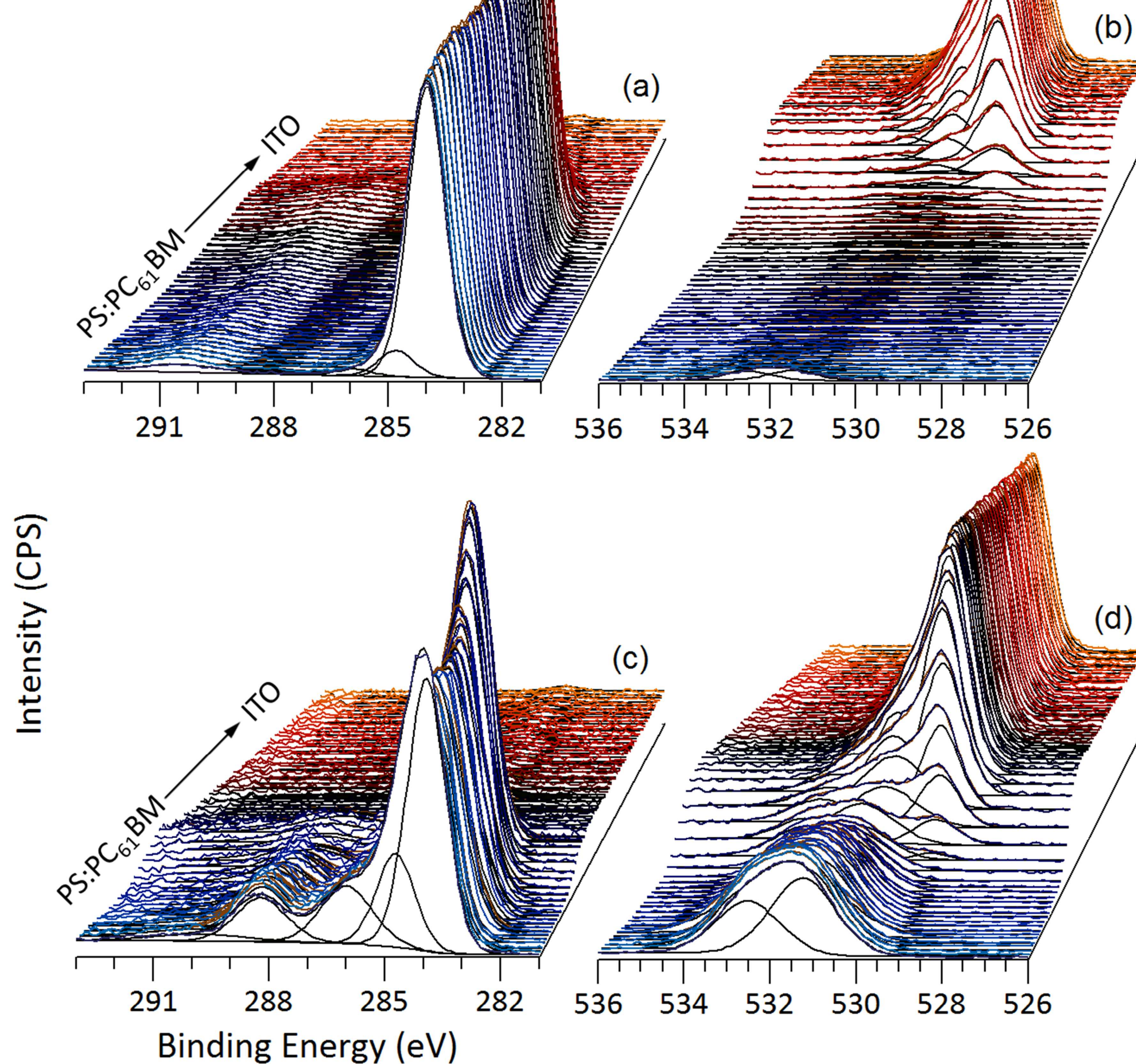

Figure 6. Typical waterfall plots through PS-$PC_{61}BM$ materials. Fresh PS-$PC_{61}BM$ (a) C(1s) envelope evolution, (b) O(1s) envelope evolution. Photo-aged PS-$PC_{61}BM$ (c) C(1s) envelope evolution, (d) O(1s) envelope evolution.

ACCE

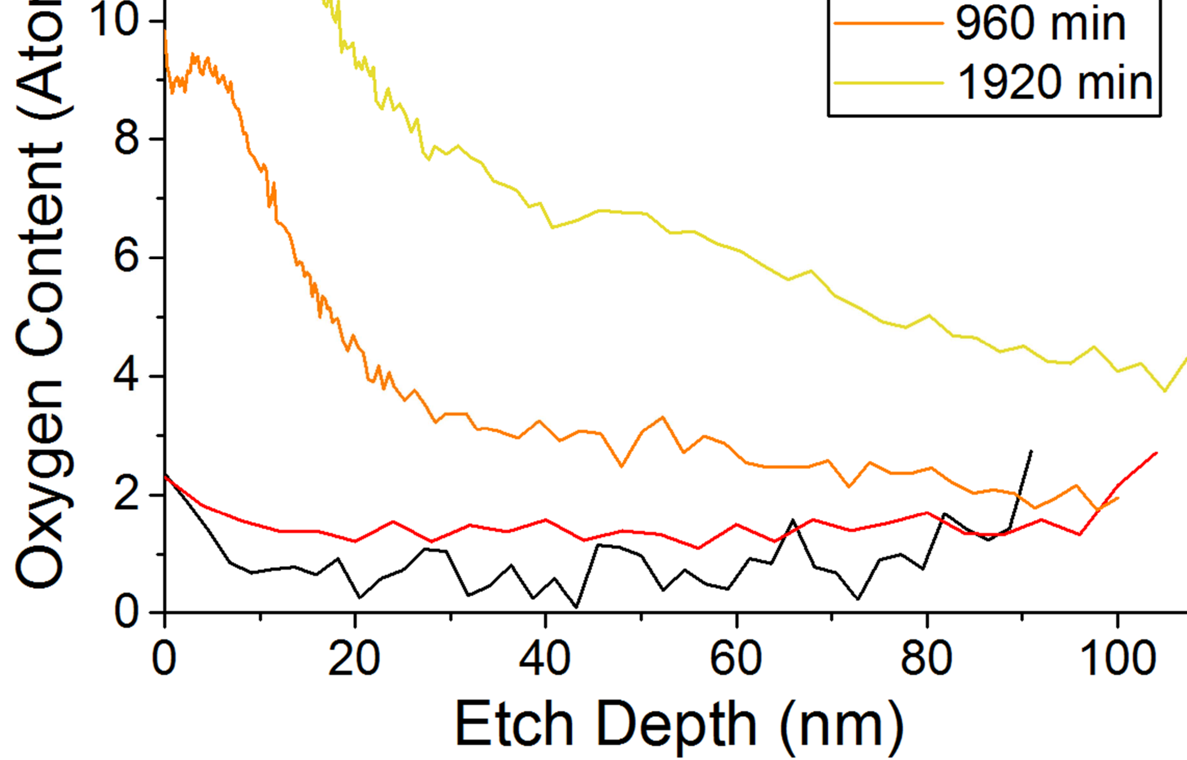

Figure 7. Evolution of oxygen within the blended film bulk as a function of exposure time to AM1.5 light.

ACCEPTED M

allows high resolution XPS envelopes to be studied at all depths. The oxygen migration through an organic material has been monitored as a function of time during film degradation. Counter-intuitively, mixing the relatively photo-stable materials PS and $PC_{61}BM$ results in a much less stable film that photo-oxidises into the bulk rather than only at the extreme surface and indicates the potential for GCIS-XPS to extend depth profiling studies even to fragile oxidised organic systems.

Acknowledgments

The authors would like to acknowledge funding from: Welsh Assembly Government funded Sêr Cymru Solar Project, EPSRC and Innovate for supporting this work through the SPECIFIC Innovation and Knowledge Centre (EP/N020863/1), and the Sêr Cymru national research network in Advanced Engineering Materials.

ACCEPTED MANUSCRIPT

Bradley, A. Manz, N. Graber, H.M. Widmer, D.R. Reyes, D. Iossifidis, P.A. Auroux, A. Manz, P. Fletcher, K.N. Andrew, A.C. Calokerinos, S. Forbes, P.J. Worsfold, Z.Y. Zhang, S.C. Zhang, X.R. Zhang, A.M. Garcia-Campana, W.R.G. Baeyens, X.R. Zhang, E. Smet, G. Van der Weken, K. Nakashima, A.C. Calokerinos, K. Tsukagoshi, M. Hashimoto, R. Nakajima, A. Arai, B.F. Liu, M. Ozaki, Y. Utsumi, T. Hattori, S. Terabe, J. Yakovleva, R. Davidsson, M. Bengtsson, T. Laurell, J. Emneus, T. Richter, L.L. Shultz-Lockyear, R.D. Oleschuk, U. Bilitewski, D.J. Harrison, S.D. Mangru, D.J. Harrison, T. Kamidate, T. Kaide, H. Tani, E. Makino, T. Shibata, R.G. Su, J.M. Lin, F. Qu, Z.F. Chen, Y.H. Gao, M. Yamada, J.G. Lv, Z.J. Zhang, A.M. Jorgensen, K.B. Mogensen, J.P. Kutter, O. Geschke, X.R. Zhang, W.R.G. Baeyens, A.M. Garcia-Campana, J. Ouyang, D. Qin, Y.N. Xia, A.J. Black, G.M. Whitesides, B.Y. Ouyang, C.W. Chi, F.C. Chen, Q.F. Xi, Y. Yang, G. Yu, K. Pakbaz, A.J. Heeger, J. Huang, A.J. deMello, D.D.C. Bradley, J.C. deMello, O. Hofmann, P. Miller, P. Sullivan, T.S. Jones, J.C. deMello, D.D.C. Bradley, A.J. deMello, D.C. Duffy, J.C. McDonald, O.J.A. Schueller, G.M. Whitesides, P.J. Hanhela, D.B. Paul, P. Lechtken, N.J. Turro, M. Reyes-Reyes, K. Kim, D.L. Carroll, Y. Kim, S. Cook, S.M. Tuladhar, S.A. Choulis, J. Nelson, J.R. Durrant, D.D.C. Bradley, M. Giles, I. McCulloch, C.S. Ha, M. Ree, M. Stigbrand, E. Ponten, K. Irgum, K. Tsukagoshi, N. Jinno, R. Nakajima, Z.J. Zhang, D.Y. He, W. Liu, Y. Lv, Integrated thin-film polymer/fullerene photodetectors for on-chip microfluidic chemiluminescence detection, Lab Chip. 7 (2007) 58–63. doi:10.1039/B611067C.

[3] C. Waldauf, P. Schilinsky, M. Perisutti, J. Hauch, C.J. Brabec, Solution-Processed Organic n-Type Thin-Film Transistors, Adv. Mater. 15 (2003) 2084–2088. doi:10.1002/adma.200305623.

[4] M. Jørgensen, K. Norrman, F.C. Krebs, M. Jorgensen, K. Norrman, F.C. Krebs, Stability/degradation of polymer solar cells, Sol. Energy Mater. Sol. Cells. 92 (2008) 686–714. doi:10.1016/j.solmat.2008.01.005.

[5] M. Jørgensen, K. Norrman, S.A. Gevorgyan, T. Tromholt, B. Andreasen, F.C. Krebs, Stability of Polymer Solar Cells, Adv. Mater. 24 (2012) 580–612. doi:10.1002/adma.201104187.

[6] W.R. Mateker, M.D. Mcgehee, Progress in Understanding Degradation Mechanisms and Improving Stability in Organic Photovoltaics, (2017) 14–16. doi:10.1002/adma.201603940.

[7] K. Norrman, M. V Madsen, S.A. Gevorgyan, F.C. Krebs, V. Frederiksborg, D.-Roskilde, Degradation Patterns in Water and Oxygen of an Inverted Polymer Solar Cell, J. Am.Chem. Soc. 132 (2010) 16883–16892. doi:10.1021/ja106299g.

[8] S. Rafique, S.M. Abdullah, K. Sulaiman, M. Iwamoto, Layer by layer characterisation of the degradation process in PCDTBT:PC71BM based normal architecture polymer solar cells, Org. Electron. 40 (2016) 65–74. doi:10.1016/j.orgel.2016.10.029.

[9] J. Kettle, Z. Ding, M. Horie, G.C. Smith, XPS analysis of the chemical degradation of PTB7 polymers for organic photovoltaics, Org. Electron. 39 (2016) 222–228. doi:10.1016/j.orgel.2016.10.016.

[10] S. Chambon, A. Rivaton, J.L. Gardette, M. Firon, Photo- and thermal degradation of MDMO-PPV:PCBM blends, Sol. Energy Mater. Sol. Cells. 91 (2007) 394–398.

ACCEPTED MANUSCRIPT

[12] S. Yamane, J. Mizukado, Y. Suzuki, M. Sakurai, L. Chen, H. Suda, MALDI-TOF MS study of the photo-oxidation of PCBM and its suppression by P3HT, Chem. Lett. (2015) 339–341. doi:10.1246/cl.141025.

[13] F. Liu, Y. Gu, J.W. Jung, W.H. Jo, T.P. Russell, On the morphology of polymer-based photovoltaics, J. Polym. Sci. Part B Polym. Phys. 50 (2012) 1018–1044. doi:10.1002/polb.23063.

[14] A. Kumar, Z. Hong, S. Sista, Y. Yang, The critical role of processing and morphology in determining degradation rates in polymer solar cells, Adv. Energy Mater. 1 (2011) 124–131. doi:10.1002/aenm.201000030.

[15] L. Ciammaruchi, F. Brunetti, I. Visoly-Fisher, Solvent effects on the morphology and stability of PTB7:PCBM based solar cells, Sol. Energy. 137 (2016) 490–499. doi:10.1016/j.solener.2016.08.018.

[16] W.R. Mateker, T. Heumueller, R. Cheacharoen, I.T. Sachs-Quintana, M.D. McGehee, J. Warnan, P.M. Beaujuge, X. Liu, G.C. Bazan, Molecular Packing and Arrangement Govern the Photo-Oxidative Stability of Organic Photovoltaic Materials, Chem. Mater. 27 (2015) 6345–6353. doi:10.1021/acs.chemmater.5b02341.

[17] J. Kettle, H. Waters, Z. Ding, M. Horie, G.C. Smith, Chemical changes in PCPDTBT:PCBM solar cells using XPS and TOF-SIMS and use of inverted device structure for improving lifetime performance, Sol. Energy Mater. Sol. Cells. 141 (2015) 139–147. doi:http://dx.doi.org/10.1016/j.solmat.2015.05.016.

[18] A. Tournebize, P.O. Bussiere, A. Rivaton, J.L. Gardette, H. Medlej, R.C. Hiorns, C. Dagron-Lartigau, F.C. Krebs, K. Norrman, New Insights into the Mechanisms of Photodegradation/Stabilization of P3HT:PCBM Active Layers Using Poly(3-hexyl-d(13)-Thiophene), Chem. Mater. 25 (2013) 4522–4528. doi:10.1021/cm402193y.

[19] I. Deckman, M. Moshonov, S. Obuchovsky, R. Brener, G.L. Frey, Spontaneous interlayer formation in OPVs by additive migration due to additive–metal interactions, J. Mater. Chem. A. 2 (2014) 16746–16754. doi:10.1039/C4TA03912B.

[20] K. Lee, P. Schwenn, A.R.G. Smith, H. Cavaye, P.E. Shaw, M. James, K.B. Krueger, I.R. Gentle, P. Meredith, P.L. Burn, Vertical morphology in solution-processed organic solar cells, IQEC/CLEO Pacific Rim. (2011) 1130–1132. http://www.opticsinfobase.org/abstract.cfm?uri=IQEC-2011-I1016 (accessed April 3, 2014).

[21] K.H. Lee, P.E. Schwenn, A.R.G. Smith, H. Cavaye, P.E. Shaw, M. James, K.B. Krueger, I.R. Gentle, P. Meredith, P.L. Burn, Morphology of all-solution-processed “bilayer” organic solar cells., Adv. Mater. 23 (2011) 766–70. doi:10.1002/adma.201003545.

[22] M.A. Ibrahem, H.-Y. Wei, M.-H. Tsai, K.-C. Ho, J.-J. Shyue, C.W. Chu, Solution-processed zinc oxide nanoparticles as interlayer materials for inverted organic solar cells, Sol. Energy Mater. Sol. Cells. 108 (2013) 156–163. doi:10.1016/j.solmat.2012.09.007.

ACCEPTED MANUSCRIPT

[24] H. Hintz, H. Peisert, Reversible and irreversible light-induced p-doping of P3HT by oxygen studied by photoelectron spectroscopy (XPS/UPS), J. Phys. …. (2011) 13373–13376. http://pubs.acs.org/doi/abs/10.1021/jp2032737 (accessed April 3, 2014).

[25] Y.K. Kyoung, H.I. Lee, J.G. Chung, S. Heo, J.C. Lee, Y.J. Cho, H.J. Kang, Damage profiles of Si (001) surface via Ar cluster beam sputtering, Surf. Interface Anal. 45 (2013) 150–153. doi:10.1002/sia.4917.

[26] J. Duchoslav, M. Arndt, R. Steinberger, T. Keppert, G. Luckeneder, K.H. Stellnberger, J. Hagler, C.K. Riener, G. Angeli, D. Stifter, Nanoscopic view on the initial stages of corrosion of hot dip galvanized Zn–Mg–Al coatings, Corros. Sci. 83 (2014) 327–334. doi:10.1016/j.corsci.2014.02.027.

[27] F.Y. Xie, L. Gong, X. Liu, Y.T. Tao, W.H. Zhang, S.H. Chen, H. Meng, J. Chen, XPS studies on surface reduction of tungsten oxide nanowire film by Ar + bombardment, J. Electron Spectros. Relat. Phenomena. 185 (2012) 112–118. doi:10.1016/j.elspec.2012.01.004.

[28] T. Miyayama, N. Sanada, S.R. Bryan, J.S. Hammond, M. Suzuki, Removal of Ar+ beam-induced damaged layers from polyimide surfaces with argon Gas Cluster Ion Beams, Surf. Interface Anal. 42 (2010) 1453–1457. doi:10.1002/sia.3675.

[29] R. Rösch, D.M.. Tanenbaum, M. Jørgensen, M. Seeland, M. Bärenklau, M. Hermenau, E. Voroshazi, M.T. Lloyd, Y. Galagan, B. Zimmermann, U. Würfel, M. Hösel, H.F. Dam, S. a. Gevorgyan, S. Kudret, W. Maes, L. Lutsen, D. Vanderzande, R. Andriessen, G. Teran-Escobar, M. Lira-Cantu, A. Rivaton, G.Y. Uzunoğlu, D. Germack, B. Andreasen, M. V. Madsen, K. Norrman, H. Hoppe, F.C. Krebs, Investigation of the degradation mechanisms of a variety of organic photovoltaic devices by combination of imaging techniques—the ISOS-3 inter-laboratory collaboration, Energy Environ. Sci. 5 (2012) 6521. doi:10.1039/c2ee03508a.

[30] I. Yamada, Materials processing by gas cluster ion beams, Mater. Sci. Eng. R Reports. 34 (2001) 231–295. doi:10.1016/S0927-796X(01)00034-1.

[31] B. Czerwinski, L. Rzeznik, R. Paruch, B.J. Garrison, Z. Postawa, Effect of impact angle and projectile size on sputtering efficiency of solid benzene investigated by molecular dynamics simulations, Nucl. Instruments Methods Phys. Res. Sect. B Beam Interact. with Mater. Atoms. 269 (2011) 1578–1581. doi:10.1016/j.nimb.2010.12.026.

[32] P.J. Cumpson, J.F. Portoles, N. Sano, Observations on X-ray enhanced sputter rates in argon cluster ion sputter depth profiling of polymers, Surf. Interface Anal. 45 (2013) 601–604. doi:10.1002/sia.5198.

[33] A.G. Shard, R. Havelund, M.P. Seah, S.J. Spencer, I.S. Gilmore, N. Winograd, D. Mao, T. Miyayama, E. Niehuis, D. Rading, R. Moellers, Argon Cluster Ion Beams for Organic Depth Profiling : Results from a VAMAS Interlaboratory Study, Anal. Chem. 84 (2012) 7865–7873.

[34] S. Surana, T. Conard, C. Fleischmann, J.G. Tait, J.P. Bastos, E. Voroshazi, R. Havelund, M. Turbiez, P. Louette, A. Felten, C. Poleunis, A. Delcorte, W. Vandervorst,

ACCEPTED MANUSCRIPT

photophysics of high open-circuit voltage, low band gap all-polymer solar cells, Energy Environ. Sci. 8 (2015) 332–342. doi:10.1039/C4EE03059A.

[36] M. Nagai, H. Wei, Y. Yoshida, Thermally induced vertical phase separation and photovoltaic characteristics of polymer solar cells for P3HT/PCBM composites, Jpn. J. Appl. Phys. 55 (2016). doi:10.7567/JJAP.55.061601.

[37] Y. Busby, E.J.W. List-Kratochvil, J.-J. Pireaux, Chemical Analysis of the Interface in Bulk-Heterojunction Solar Cells by X-ray Photoelectron Spectroscopy Depth Profiling, ACS Appl. Mater. Interfaces. 9 (2017) 3842–3848. doi:10.1021/acsami.6b14758.

[38] D.-J. Yun, J. Kim, J. Chung, S. Park, W. Baek, Y. Kim, S. Kim, Y.-N. Kwon, J. Chung, Y. Kyoung, K.-H. Kim, S. Heo, Study on the chemical stability of catalyst counter electrodes for dye-sensitized solar cells using a simple X-ray photoelectron spectroscopy-based method, J. Power Sources. 268 (2014) 25–36. doi:10.1016/j.jpowsour.2014.06.011.

[39] D.-J. Yun, J. Chung, C. Jung, K.-H. Kim, W. Baek, H. Han, B. Anass, G.-S. Park, S.-H. Park, An electronic structure reinterpretation of the organic semiconductor/electrode interface based on argon gas cluster ion beam sputtering investigations, J. Appl. Phys. 114 (2013) 13703. doi:10.1063/1.4812582.

[40] D.-J. Yun, J. Chung, C. Jung, Y. Chung, S. Kim, S. Lee, K.-H. Kim, H. Han, G.-S. Park, S. Park, A novel approach for the characterization of a bilayer of phenyl-c71-butyric-acid-methyl ester and pentacene using ultraviolet photoemission spectroscopy and argon gas cluster ion beam sputtering process, J. Appl. Phys. 114 (2013) 94510. doi:10.1063/1.4820393.

[41] J. Haberko, M.M. Marzec, A. Bernasik, W. Łużny, P. Lienhard, A. Pereira, J. Faure-Vincent, D. Djurado, A. Revaux, XPS depth profiling of organic photodetectors with the gas cluster ion beam, J. Vac. Sci. Technol. B, Nanotechnol. Microelectron. Mater. Process. Meas. Phenom. 34 (2016) 03H119. doi:10.1116/1.4943028.

[42] R. Dattani, J.T. Cabral, Polymer fullerene solution phase behaviour and film formation pathways., Soft Matter. 11 (2015) 3125–31. doi:10.1039/c5sm00053j.

[43] G. Bernardo, N. Deb, S.M. King, D.G. Bucknall, Phase behavior of blends of PCBM with amorphous polymers with different aromaticity, J. Polym. Sci. Part B Polym. Phys. 54 (2016) 994–1001. doi:10.1002/polb.24002.

[44] L. Zheng, J. Liu, Y. Sun, Y. Ding, Y. Han, Manipulating the crystallization of methanofullerene thin films with polymer additives, Macromol. Chem. Phys. 213 (2012) 2081–2090. doi:10.1002/macp.201200341.

[45] A.N. Cha, Y. Ji, S.A. Lee, Y.Y. Noh, S.I. Na, S. Bae, S. Lee, T.W. Kim, Fabrication of spray-printed organic non-volatile memory devices for low cost electronic applications, Mater. Sci. Eng. B Solid-State Mater. Adv. Technol. 191 (2015) 51–56. doi:10.1016/j.mseb.2014.10.010.

[46] J. Shi, W. Zhou, L. Zhang, K. Hu, Y. Xie, Morphology, structure, and photovoltaic properties of poly(3-hexylthiophene) and [6,6]-phenyl-C61-butyric acid methyl ester-based ternary blends doping with polystyrene of different tacticities, J. Appl. Polym.

ACCEPTED MANUSCRIPT

doi:10.1039/C4TA05309E.

[48] L.A. Matheson, R.F. Boyer, Light Stability of Polvstyrene and Polyvinylidene Chloride, Ind. Eng. Chem. 44 (1952) 867–874.

[49] M.H. Richter, D. Friedrich, D. Schmeißer, Valence and Conduction Band States of PCBM as Probed by Photoelectron Spectroscopy at Resonant Excitation, Bionanoscience. 2 (2012) 59–65. doi:10.1007/s12668-011-0034-1.

[50] I.E. Brumboiu, L. Ericsson, R. Hansson, E. Moons, O. Eriksson, B. Brena, The influence of oxygen adsorption on the NEXAFS and core-level XPS spectra of the C60 derivative PCBM., J. Chem. Phys. 142 (2015) 54306. doi:10.1063/1.4907012.

[51] M.O. Reese, A.M. Nardes, B.L. Rupert, R.E. Larsen, D.C. Olson, M.T. Lloyd, S.E. Shaheen, D.S. Ginley, G. Rumbles, N. Kopidakis, Photoinduced degradation of polymer and polymer-fullerene active layers: Experiment and theory, Adv. Funct. Mater. 20 (2010) 3476–3483. doi:10.1002/adfm.201001079.

[52] Z. Xiao, J. Yao, D. Yang, F. Wang, S. Huang, L. Gan, Z. Jia, Z. Jiang, X. Yang, B. Zheng, G. Yuan, S. Zhang, Z. Wang, Synthesis of [59]fullerenones through peroxide-mediated stepwise cleavage of fullerene skeleton bonds and X-ray structures of their water-encapsulated open-cage complexes, J. Am. Chem. Soc. 129 (2007) 16149–16162. doi:10.1021/ja0763798.

[53] S. Krimm, Infrared spectra of high polymers, Adv. Polym. Sci. 2 (1960) 51–172. doi:10.1016/0022-2852(59)90048-7.

[54] T. Miyayama, Practical Applications of Argon Gas Cluster Ion Beam for ray Photoelectron Spectroscopy and Time-of-flight Secondary Ion Mass Spectrometry, J. Vac. Soicety Japan. 56 (2013) 348–354.

[55] F.C. Krebs, K. Norrman, Analysis of the Failure Mechanism for a Stable Organic Photovoltaic During 10000h of Testing, Prog. Photovolt Res. Appl. 15 (2007) 697–712. doi:10.1002/pip.

[56] S. Shoaee, J.R. Durrant, Oxygen diffusion dynamics in organic semiconductor films, J. Mater. Chem. C. 3 (2015) 10079–10084. doi:10.1039/C5TC02822A.

ACCEPTED MANUSCRIPT

- The scale of oxidation is observed to increase when PCBM is blended with a stable polymer.
- Stability of PCBM to gas cluster ion source etching is demonstrated.
- Depth profiling confirms that oxidation penetrates into the bulk for PCBM-polymer blends.

ACCEPTED MANUSCRIPT